THE PROLONGED WEATHERING OF IRON AND STONY-IRON METEORITES AND THEIR ANOMALOUS CONTRIBUTION TO THE AUSTRALIAN REGOLITH

DAVID B TILLEY[1] AND ALEX W R BEVAN[2]

[1]*Cooperative Research Centre for Landscape Evolution and Mineral Exploration*
Australian National University, Canberra ACT 0200, Australia
[2] *Department of Earth and Planetary Sciences*
Western Australian Museum, Perth WA 6000, Australia

ABSTRACT

The surface of the Earth has been bombarded continually by meteorites since it first accreted 4 6 billion years ago Australia's relative tectonic stability and prolonged aridity has provided an ideal site for the accumulation of meteorites over a long period of time, so much so that the Nullarbor Plain in southern Australia is considered one of the best collecting grounds for meteorites after Antarctica Unlike those from Antarctica, portions of some ancient Australian iron meteorites have become so highly weathered (either in part or in whole) that fragmental material has come to resemble much of the ferruginous lag that blankets many parts of arid Australia Herein lies the difficulty those mineral exploration companies searching for nickel and platinum group elements (PGE) face Is ferruginous sample media anomalously high in these economic minerals, derived from deep weathering of ore-bearing ultramafic rock or are they the scattered remnants of highly weathered iron-nickel meteorites which are of virtually no economic value other than to academics and collectors? To address this confusion, highly weathered portions of 3 iron meteorites and 1 pallasite were characterised using a variety of analytical techniques so that the origin of suspect ferruginous sampling media found during geochemical exploration could be determined

Key words: geochemical exploration, iron meteorite, laterite, nickel, pallasite, platinum, ultramafic weathering

BACKGROUND

Approximately 5% of meteorites that fall on the Earth are the metallic Fe-Ni variety (Bevan, 1992) and are termed "iron meteorites" Such meteorites are mainly composed of the minerals kamacite (∝-(Fe,Ni), Ni<7 5%) and taenite (γ-(Fe,Ni), Ni>25%) Secondary minerals formed by the corrosion of metallic Fe-Ni include, akaganéite (ß-FeO(OH,Cl)), bunsenite (NiO), goethite (∝-FeO(OH)), hematite (∝-Fe_2O_3), hibbingite (γ-$Fe_2(OH)_3Cl$), lepidocrocite (γ-FeO(OH), maghemite (γ-Fe_2O_3), magnetite (Fe_3O_4) and trevorite ($NiFe_2O_4$) (Rubin, 1997) Buchwald and Clarke (1989) showed that the corrosion of metal in meteorites passes through an intermediate step with the precipitation of Cl-containing akaganéite near the reaction front Chloride ions incorporated within ion-exchange sites within the tunnel structure of akaganéite may be retained, made available for the assistance of corrosion or flushed entirely from the system As akaganéite ages it transforms into mainly goethite and maghemite (Buchwald and Clarke, 1989) Other researchers in the field include Golden et al (1995) and White et al (1967) Golden et al (1995) studied the oxidation products on the surface of the Hoba iron-nickel meteorite found in Namibia White et al (1967) examined secondary minerals produced during weathering of the Wolf Creek meteorite found in Australia and discovered two new minerals; reevesite ($Ni_6Fe_2(OH)_{16}CO_3\ 4H_2O$) and cassidyite ($Ca_2(Ni,Mg)(PO_4)_2\ 2H_2O$) The Wolf Creek meteorite was determined to have a terrestrial age of 300,000 years (Shoemaker, 1990)

IMPLICATIONS FOR LANDSCAPE EVOLUTION AND MINERAL EXPLORATION

Ferruginous lag is residual material derived from the intense lateritic weathering of underlying iron-rich bedrock When transported, as in sheet wash and by streams, lag becomes geochemically unrelated to the underlying rock It is commonly used as a sampling medium because the component iron oxides and oxyhydroxides are extremely good trace element scavengers Although certain trace elements may be uneconomic, when correlated with economic ones such as Au, Ni and Pt, they become useful as pathfinder elements for detecting ore deposits Sampling of lag is normally carried out with a dustpan and broom, however

when scarce, ferruginous material may be simply picked off the land or detected with a metal detector. Ferruginous lag derived from the weathering of ultramafic rocks and material derived from the corrosion of iron meteorites is virtually identical in appearance. Scarce ferruginous lag containing anomalously high amounts of siderophile elements should be investigated further to discount the possibility that the sample had an extraterrestrial origin. The anomalous geochemical contribution of meteorites to the Australian landscape is not well understood and is rarely taken into account by the mineral exploration industry. It however becomes a plausible consideration when considering that the flux of meteorites in the range 10g to 1kg over the entire Earth's surface is between 2900kg and 7300kg per year (Bland et al. 1996). The antiquity of the Australian landscape is another important consideration. Small highly weathered meteorites should theoretically be plentiful, however their similar appearance to ordinary ferruginous lag makes them extremely difficult to identify in the field. Structures caused by the impact of large meteorites are however more obvious and they themselves can be economically significant. Up to a quarter of known large impact structures are associated with economic resources, including metalliferous mineral deposits such as the Ni-Cu ores of Sudbury, Ontario, Canada and the Witwatersrand gold deposits located in the ring structural depression of the Vredefort impact structure, South Africa (Glikson, 1996).

Experimental Method

Highly weathered portions of the Mundrabilla, Youndegin and Wolf Creek iron meteorites, as well as parts of the Huckitta stony-iron were obtained from the Western Australian Museum. Table 1 outlines some important characteristics of these meteorites.

A few grams of each portion was crushed and milled in a tungsten carbide ring-mill. To 0.8 g of each milled sample was added 0.2 g of zincite (ZnO) to facilitate the quantification of poorly diffracting material (PDM). PDM is generally composed of crystals less than 10 nm in size where the small number of layers within such crystals result in X-ray diffraction (XRD) patterns which have very weak and broad diffraction maxima. Diffraction is generally so poor that information in the XRD pattern is lost in the background noise. Material of a larger size that lacks or has no internal crystalline structure and is commonly referred to as amorphous material, may also be included as PDM in the analyses. For simplicity, this paper does not differentiate between amorphous and poorly diffracting materials and all such materials are included under the one term. PDM dilutes the overall diffracting power of the sample resulting in an increase in the ZnO content with respect to the well-diffracting phases. This property was used by SIROQUANT™, a quantitative XRD phase analysis program written by Taylor and Clapp (1992) to calculate the quantity of PDM in each of the samples. CoKα radiation was used to minimise the absorption contrast between the iron-bearing minerals and the ZnO.

Milled portions that were analysed by XRD were submitted to INAX Services for major and trace element analysis by X-ray fluorescence spectroscopy (XRF). PGE and Au were analysed by ANALABS using a lead collection fire assay technique followed by inductively coupled plasma mass-spectrometry (ICP-MS). Youndegin was not analysed for PGE and Au because the minimum quantity of 30 g required for analysis could not be obtained.

The remaining unmilled portion of each meteorite was sectioned and polished on a tin lap with diamond paste. Reflected light microscopy was used to highlight variations in mineral reflectivity and texture across the polished surface. Back-scattered electron microscopy (SEM) and energy dispersive X-ray analysis (EDXA) were performed on grains and regions of similar back-scattered electron intensity to analyse and identify them.

Results

SIROQUANT™ revealed the mineralogy of the weathered meteorites including the amount of PDM present (Table 2). Huckitta's mineralogy was recalculated to exclude forsterite (which amounted to 15.1 wt.%) so that a direct comparison could be made with the other three meteorites without the diluting effect of the forsterite. After the correction was made, the two most dominant phases present in the weathered meteorites were maghemite (av. 45.8 wt.%) and goethite (av. 30.0 wt.%). The detection of hematite was somewhat conjectural due to the main 2.70 Å peak interfering with the 2.69 Å peak of goethite. For this reason, it was decided to utilise SIROQUANT(™)'s in-built peak deconvolution ability to automatically determine the hematite content. Using this method, the average hematite content of the weathered meteorites was determined to be 3.8 wt.%. Lepidocrocite was a relatively easy mineral to detect in all of the weathered meteorites, even though it averaged only 2.5 wt.%. This was due principally to its main diffraction peak at 6.26 Å

being far removed from the interfering effects of other peaks. Quartz content ranged from 0.3 to 1.5 wt %, with an average of 0.9 wt %. An interesting outcome of the XRD analysis was the significant amount of poorly diffracting material found within the meteorites. PDM ranges from 12.2 wt.% in Youndegin to 24.4 wt.% in Huckitta (recalculated). When considering that the detection limit for PDM analysis is approximately 5 wt %, an average PDM content of 17.0 wt % is quite significant when considering that just a few years ago such material was commonly ignored due to the difficulty in quantifying it.

Results of the major and trace element analysis of the samples are outlined in Table 3 and 4. Data from the trace element analysis of Mundrabilla, Youndegin and Wolf Creek were averaged and plotted against the average trace element abundance of the corresponding unweathered meteorites obtained from Buchwald (1975). The resultant graph (Figure 1) showed that all the elements except Cr were of a lower abundance in the weathered meteorites than in the unweathered. Figure 2 and Table 5 display a comparison between the average, minimum and maximum abundance of PGE and Au in the weathered iron meteorites and the abundance of these elements in 46 unweathered iron meteorites studied by Crocket (1972). For comparison, Table 6 displays the average, minimum and maximum abundance of PGE and Au in 41 unweathered iron meteorites studied by Pernicka and Wasson (1987). Figure 2 shows that the abundance of PGE and Au in the weathered iron meteorites is lower than the average abundance in the unweathered iron meteorites. However, the abundances still fall within the overall range except for Os in Wolf Creek and Au in Huckitta and Mundrabilla. As the analyses of the unweathered meteorites have a range of values, a direct comparison was made in Table 5 between weathered and unweathered Mundrabilla (Pernicka and Wasson, 1987). The comparison showed that the PGE and Au abundance in the weathered sample were lower than in the unweathered sample of Pernicka and Wasson (1987).

Polished sections of the weathered meteorites were imaged using reflected light microscopy and SEM. Unaltered primary minerals were easily recognised as having a higher reflectivity in reflected light and a greater intensity in SEM. Primary minerals detected include kamacite (α-(Fe,Ni)) in Youndegin (Figure 3a), taenite (γ-(Fe,Ni)) in Mundrabilla and Wolf Creek (Figure 3b) and cohenite ($(Fe,Ni)_3C$) in Youndegin (Figure 4). EDAX of material at the weathering front in cohenite (arrowed in Figure 3c) indicated the presence of Cl-bearing akaganéite (β-(Fe,Ni)O(OH,Cl)). The primary mineral schreibersite ($(Fe,Ni)_3P$) was detected in all specimens (Figures 3d, 3e and 5). The weathered material surrounding schreibersite particles (arrowed in Figure 3d) was determined to have a composition of arupite-vivianite ($(Fe,Ni)_3(PO_4)_2\ 8H_2O$). Forsterite in the Huckitta pallasite was brecciated, however was virtually unweathered (Figure 6). EDAX showed that some bright patches in Wolf Creek (Figure 3f) were composed of barite ($Ba,Sr(SO_4)$). The majority of the weathered material is composed of nickeliferous iron oxides and oxyhydroxides; mainly maghemite (γ-$(Fe,Ni)_2O_3$) and goethite (α-(Fe,Ni)O(OH)), both of which were easily distinguished in the polished sections.

INTERPRETATION

Chemical analyses using EDAX of the goethite and maghemite indicate that substitution of Fe for Ni is common. Weathering of kamacite to nickeliferous maghemite appears to be a pseudomorphic process leading to the partial preservation of internal structures. Very little nickel is lost during the process hence the nickel content of the maghemite is similar to that of the original alloy. Nickeliferous goethite on the other hand, was probably formed by a dissolution-precipitation mechanism. Nickel is lost from the system during this process, resulting in lower values of Ni in the goethite than in the maghemite.

The small amount of quartz detected in the weathered meteorites is anomalous because unweathered iron meteorites do not contain quartz (Buchwald, 1975). It appears that the quartz was derived from the surrounding soil and was incorporated into the weathered mass during corrosion.

The presence of PDM in weathered meteorites may be attributed to the poorly diffracting mineral ferrihydrite ($Fe_5O_7(OH)\ 4H_2O$) which is commonly produced during rusting of metallic iron. Ferrihydrite is normally difficult to detect because of its nanoscopic crystal size and the need for it to be present in sufficient quantities for its very weak diffraction maxima to become observable.
The process of geochemical dispersion from the site of weathering may explain the lower abundance of trace elements (except Cr) in the weathered samples as compared to the unweathered meteorites. Commonly, such dispersion is responsible for geochemical haloes around ore deposits. An explanation for the apparent enrichment in Cr may be attributed to the presence of chromite ($FeCr_2O_4$) in iron meteorites. Although

undetected in the SEM study, chromite has been reported to occur in Mundrabilla and occurs as small 100-200 µm grains in Wolf Creek (Bevan, pers com 1998) Chromite's resistance to weathering may result in its residual accumulation during weathering.

CONCLUSION

XRD alone is insufficient for determining the meteoritic origin of certain ferruginous materials found during geochemical exploration All minerals detected in weathered iron meteorites by XRD are common to the Earth's surface in varying amounts Perhaps the only conclusion that can be made about ferruginous material having similar mineral proportions to that of Table 2, is that it was derived from the rusting of either natural (generally meteoritic) or artificial iron The use of SEM together with EDAX however, provides evidence that is more conclusive. Remnant fragments of primary minerals such as kamacite, taenite, schreibersite and cohenite detected within the weathered masses leave little doubt as to their extraterrestrial origin. Full chemical analyses including PGE and Au also help in determining whether or not the samples were former meteorites

ACKNOWLEDGEMENTS

Samples were kindly supplied by the Western Australian Museum SEM was performed using the facilities of the Electron Microscopy Unit at the Australian National University

REFERENCES

Bevan, A W R (1992) Australian meteorites, Records of the Australian Museum Supplement 15, 1-27.

Bevan, A W R (1996) Australian crater-forming meteorites, AGSO Journal of Australian Geology & Geophysics, 16, 421-429.

Bland, P A , Smith, T B , Jull, A J T , Berry, F J , Bevan, A W R , Cloudt, S and Pillinger, C T (1996) The flux of meteorites to the Earth over the last 50,000 years, Mon. Not R Astron Soc , 283, 551-565.

Buchwald, V F (1975) Handbook of Iron Meteorites vol. 1, 2 and 3, University of California Press.

Buchwald, V F. and Clarke, R S. (1989) Corrosion of Fe-Ni alloys by Cl-containing akaganéite (β-FeOOH): The Antarctic meteorite case, The American Mineralogist, 74, 656-667

Crocket, J H. (1972) Some aspects of the geochemistry of Ru, Os, Ir and Pt in iron meteorites, Geochimica et Cosmochimica Acta, 36, 517-535

Glikson, A Y. editor (1996) Thematic issue: Australian impact structures-Preface, AGSO Journal of Australian Geology & Geophysics, 16, 371

Golden, D C., Ming, D W and Zolensky, M E. (1995) Chemistry and mineralogy of oxidation products on the surface of the Hoba nickel-iron meteorite, Meteoritics & Planetary Science, 30, 418-422.

Madigan, C.T. (1939) The Huckitta meteorite, Central Australia, Mineralogical Magazine, 25, 353-371

Pernicka, E. and Wasson, J T. (1987) Ru, Re, Os, Pt and Au in iron meteorites, Geochimica et Cosmochimica Acta, 51, 1717-1726

Rubin, A E. (1997) Mineralogy of meteorite groups, Meteoritics & Planetary Science, 32, 231-247

Shoemaker, E M , Shoemaker, C S., Nishiizumi, K , Kohl, C P , Arnold, J R , Klein, J , Fink, D , Middleton, R , Kubik, P W and Sharma, P., 1990 Ages of Australian meteorite craters: a preliminary report (abstract), Meteoritics & Planetary Science, 25, 409.

Taylor, J C. and Clapp, R A. 1992 New features and advanced applications of SIROQUANT: a personal computer XRD full profile quantitative analysis software package Advances in X-ray Analysis 35: 49-55

White, J S., Henderson, E P. and Mason, B (1967) Secondary minerals produced by weathering of the Wolf Creek meteorite, The American Mineralogist, 52, 1190-1197

Table 1: *Characteristics of the unweathered meteorites*

	Location	Type	Bandwidth	Ni %
Mundrabilla [1]	30°50'S 127°30'E	structurally anomalous medium octahedrite	0.55±0.10 mm	7.80
Huckitta [2]	22°22'S 135°46'E	pallasite	2.1 mm	8.98
Youndegin [1]	32°06'S 117°43'E [3]	coarse octahedrite	2.3±0.5 mm	6.74
Wolf Creek [1]	19°10'S 127°46'E [4]	medium octahedrite	0.85±0.15 mm	9.22

[1] Data unless otherwise specified obtained from Buchwald (1975)

[2] Data unless otherwise specified obtained from Madigan (1939); bandwidth and Ni content applies only to the metallic component

[3] Coordinates obtained from Bevan (1992)

[4] Coordinates obtained from Bevan (1996)

Table 2: *Quantitative XRD of the weathered meteorites (weight %)*

	Forsterite	Maghemite	Goethite	Lepidocrocite	Hematite	Quartz	PDM
Mundrabilla	0.0	50.1	32.1	1.5	3.4	0.4	12.4
Huckitta	15.1	38.8	21.6	1.9	2.5	1.1	19.0
recalculated	0.0	45.7	25.4	2.2	2.9	1.3	22.4
Youndegin	0.0	57.3	24.0	1.6	4.7	0.3	12.2
Wolf Creek	0.0	30.0	38.4	4.7	4.3	1.5	21.1
average	0.0	45.8	30.0	2.5	3.8	0.9	17.0

Table 3: *Major element analyses of the weathered meteorites (weight %)*

Weight %	Mundrabilla	Huckitta	Youndegin	Wolf Creek
NiO	6.291	4.978	5.038	4.461
*Co_3O_4	0.418	0.318	0.411	0.388
Fe_2O_3	83.209	69.189	87.916	81.847
MnO	0.022	0.055	0.001	0.003
Cr_2O_3	0.060	0.032	0.002	0.000
TiO_2	0.010	0.032	0.014	0.019
BaO	0.004	0.017	0.006	0.015
CaO	0.606	0.187	0.025	0.050
K_2O	0.029	0.072	0.006	0.022
SO_3	0.586	0.109	0.282	0.167
P_2O_5	0.660	0.741	0.405	0.737
SiO_2	0.809	11.101	0.530	3.181
Al_2O_3	0.169	0.868	0.149	0.431
MgO	0.110	8.214	0.000	0.038
Na_2O	0.069	0.015	0.001	0.003
Total	93.052	95.928	94.78	91.362

*Co_3O_4 analysis may be affected by milling

Table 4: *Trace element analyses of the weathered meteorites (ppm)*

PPM	MUNDRABILLA	HUCKITTA	YOUNDEGIN	WOLF CREEK
V	13 3	30.1	0	41 2
Cr	339.9	166.2	0	0
*Co	1840	1500	1550	1600
Ni	46140	39140	34990	33590
Cu	84.5	62.2	99.4	92.2
Zn	12 3	11	31 3	6.1
Ga	44 1	15 9	55 5	12.9
Ge	123.3	35	213 7	26.8
Se	0	0	1 7	0
Br	16.3	7.2	4 3	12.4
Sr	23 3	29.8	3.1	9 6
Zr	4 8	9.5	6.6	7 7
Mo	17 3	14 2	19.5	15.4
Ag	7	5 1	8.5	6 6
In	3.2	1.6	3.6	2.3
Sn	5 9	2.3	5 3	2.7
Sb	0 4	0	0 6	0
I	0	1 1	0	20.5
Ba	27.9	139.6	10.6	136 9
La	0	3	0	9 4
Ce	1 3	3.3	1 9	17 4
*W	298 2	291 2	174	238.6

*W and Co analyses may be affected by milling

Table 5: *Average, minimum and maximum PGE and Au abundance in 46 unweathered iron meteorites (data obtained from Crocket, 1972) compared with abundance in the weathered meteorites from this study Youndegin is not included due to insufficient sample for analysis Mundrabilla (weathered) is compared with the mean of replicate analyses of unweathered material from Pernicka and Wasson (1987)*

ELEMENT	AVERAGE (PPM)	MINIMUM (PPM)	MAXIMUM (PPM)	WOLF CREEK (PPM)	MUNDRABILLA (PPM) (WEATHERED)	MUNDRABILLA (PPM) (UNWEATHERED)	HUCKITTA (PPM)
Ru	7 32	0.16	36	1.4825	2.072	3.16	1.6305
Pd	4 5	1 6	19.7	2 066	2.56	-	2.372
Os	5.36	0.009	58	0.0035	0.588	0.71	0.307
Ir	3 96	0.009	47	0.014	0.534	-	0 3385
Pt	9 42	0.5	29	2.552	3 0135	3 6	3 5315
Au	1.32	0 21	3 61	0 265	0.187	1 51	0 097
Re	0.4166	0.0023	4 35	-	-	0.084	-
Rh	-	-	-	0.9155	0.6435	-	0.623

Table 6: *Average, minimum and maximum PGE and Au abundance in 41 unweathered iron meteorites from Pernicka and Wasson (1987). Palladium was not reported.*

	AVERAGE (PPM)	MINIMUM (PPM)	MAXIMUM (PPM)
Ru	7.06	0.03	26
Pd	-	-	-
Os	8.01	0.005	86
Ir	6.29	0.006	59
Pt	9.85	0.1	38
Au	1.15	0.27	2.87
Re	0.5833	0.0007	4.8

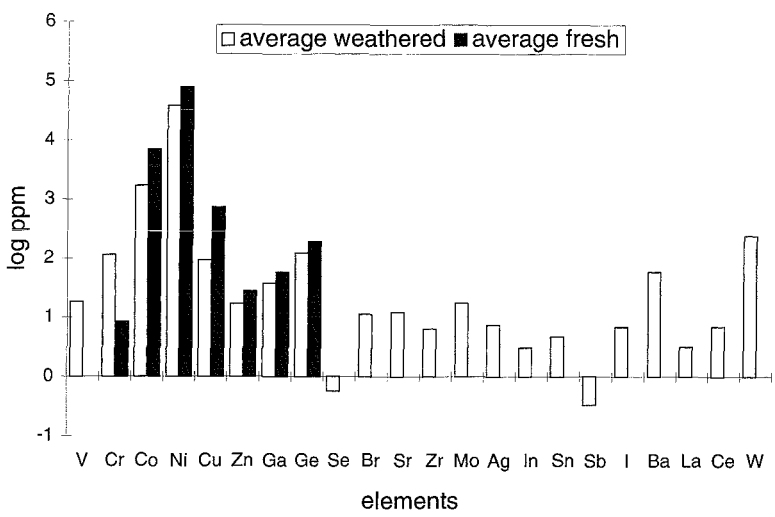

Figure 1: *Comparison between the average trace element abundance of weathered iron meteorites from this study and those of the unweathered iron meteorites from Buchwald (1975). Huckitta is excluded from the averages as the presence of forsterite may cause a discrepancy. The abundance is plotted as log10 ppm for clarity of presentation.*

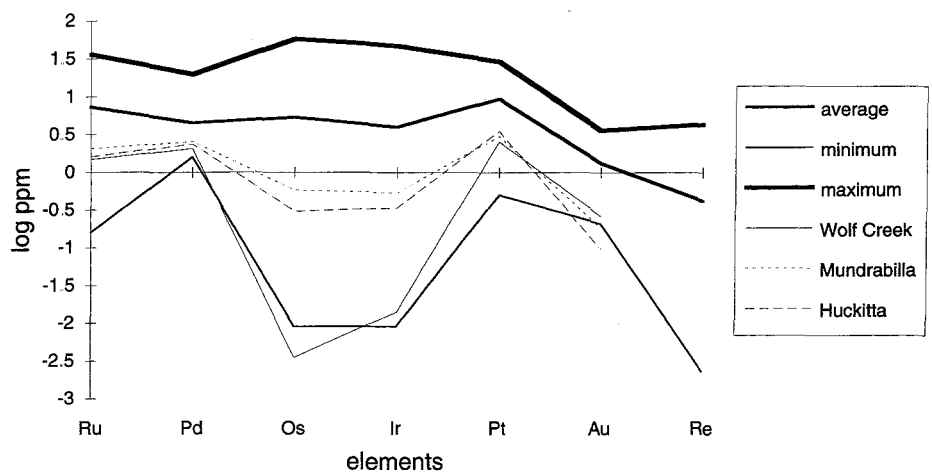

Figure 2: *PGE and Au abundance in the weathered iron meteorites compared to the minimum, maximum and average values of 46 unweathered iron meteorites from Crocket (1972). The abundance is plotted as log10 ppm for clarity of presentation.*

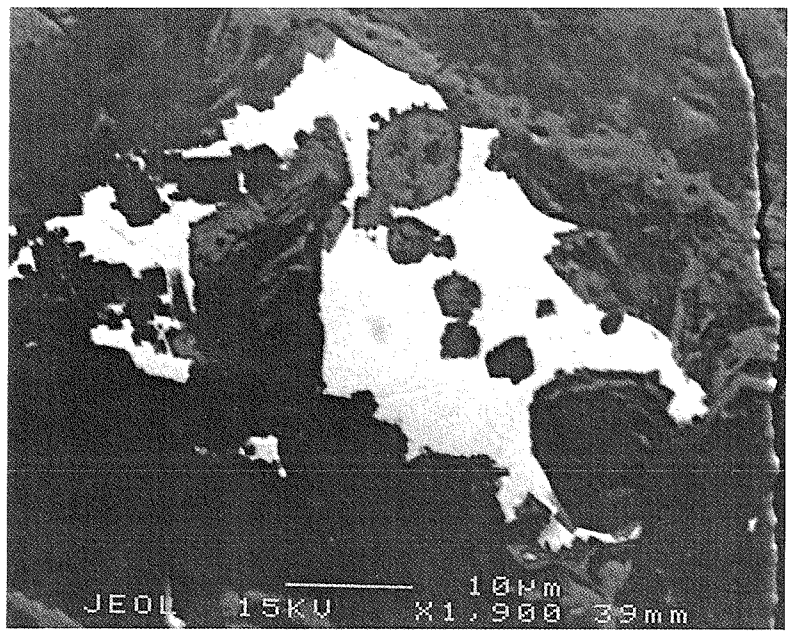

Figure 3: *Polished sections of the weathered iron meteorites imaged using back-scattered electron microscopy.*

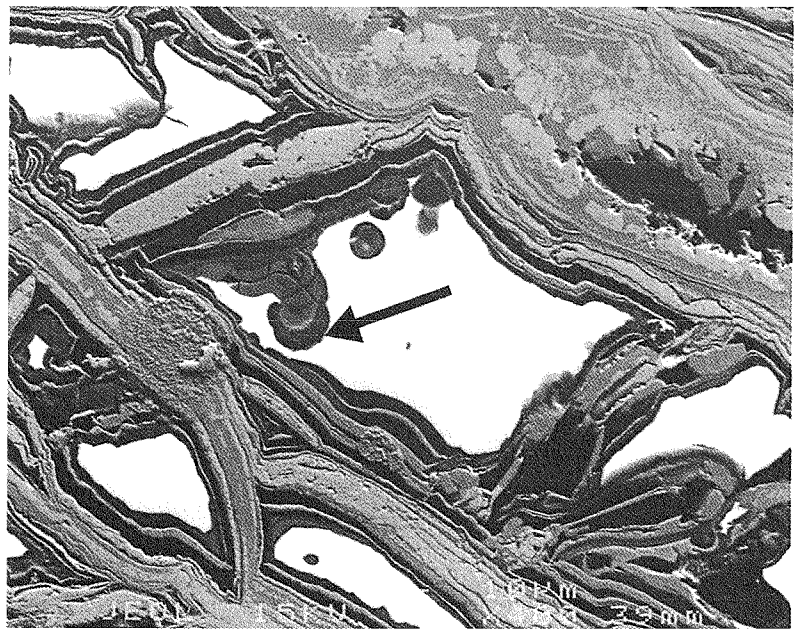

Figure 3(a): *Bright, irregular patches of unweathered kamacite in Youndegin, scale bar = 10 µm*

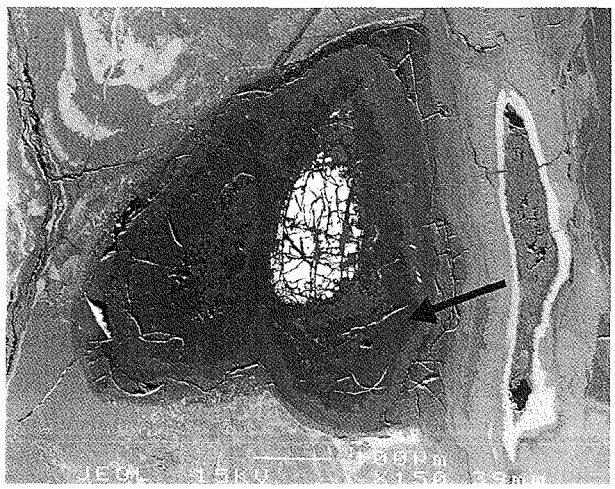

Figure 3(b): *Unweathered plessitic taenite (bright areas) in Wolf Creek, scale bar = 10 µm*

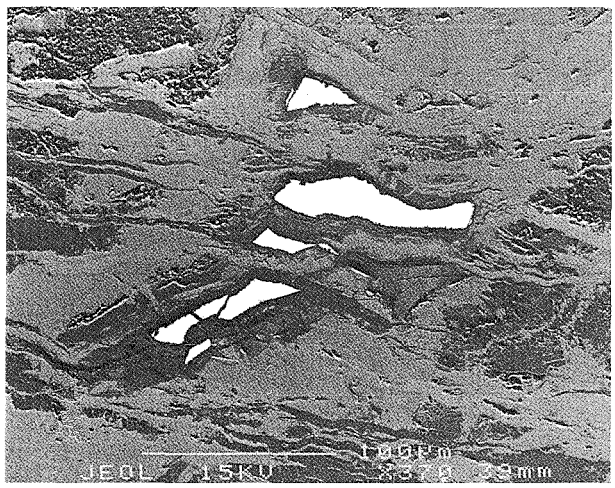

Figure 3 (c): *Fragmented and weathered cohenite (bright patches) in Youndegin, scale bar = 10 µm. Material with a composition of Cl-bearing akaganÈite is present within the embayed cohenite (arrowed)*

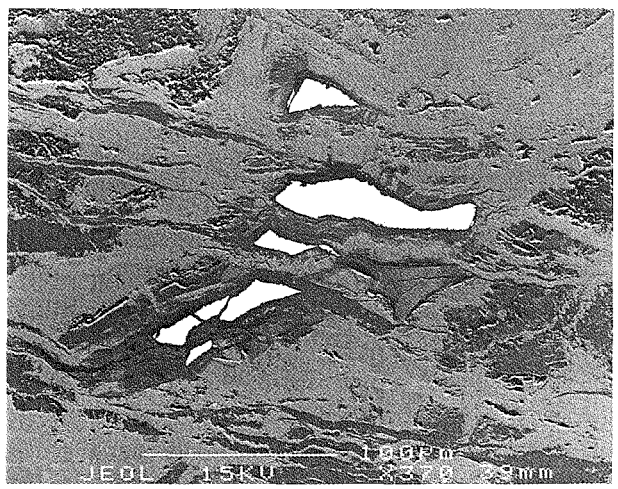

Figure 3(d): *Brecciated and weathered schreibersite (bright areas) in Wolf Creek, scale bar = 100 µm. The dark grey area surrounding the schreibersite has a composition of arupite-vivianite (arrowed)*

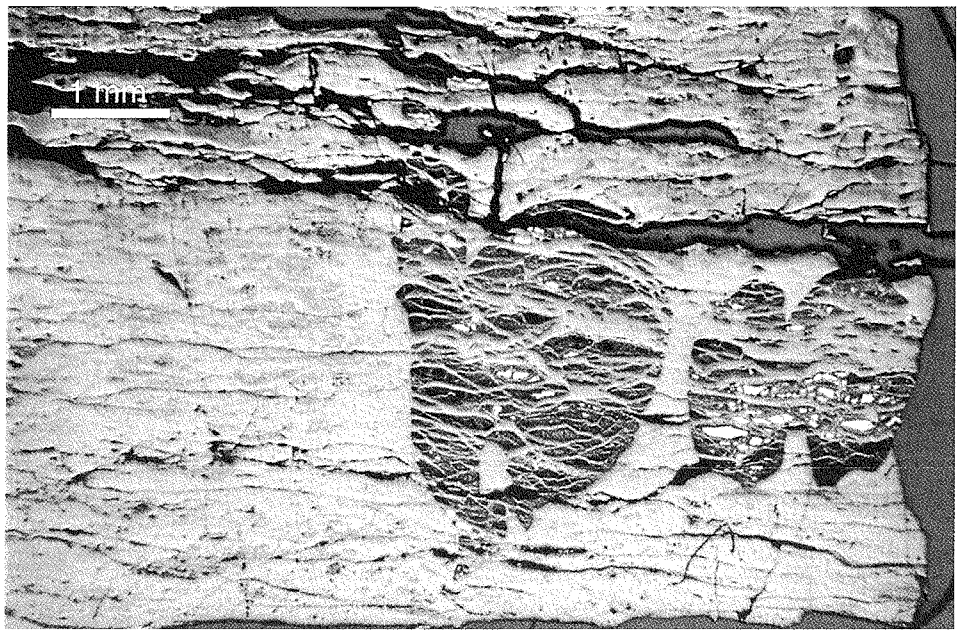

Figure 3(e): *Weathered fragments of schreibersite (bright patches) in Youndegin, scale bar = 100 μm*

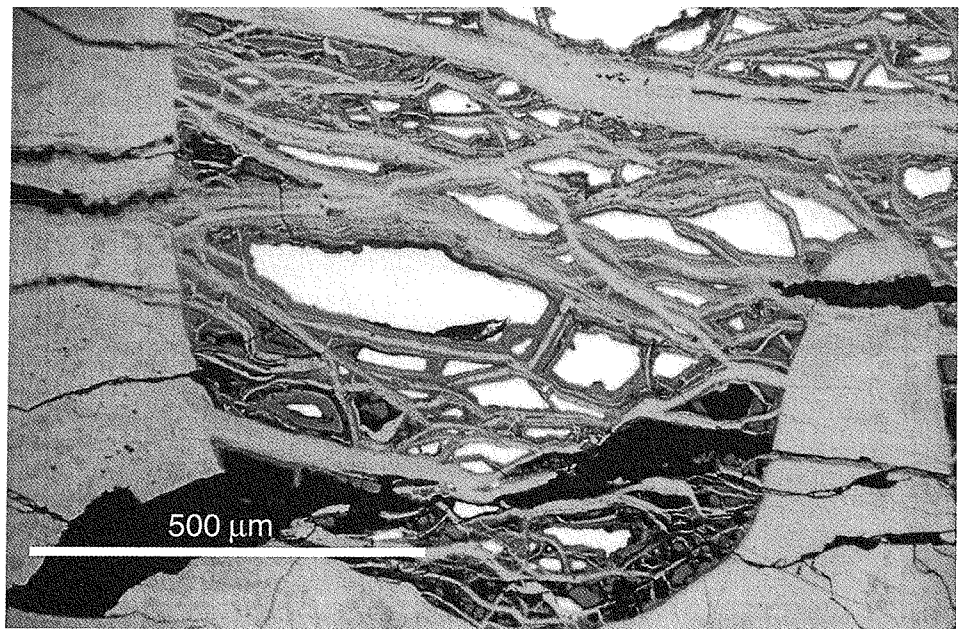

Figure 3(f): *Bright, irregular patches of barite occupying voids within the relatively dark nickeliferous goethite and maghemite of Wolf Creek; scale bar = 100 μm.*

Figure 4: *Reflected light microscopy of Youndegin showing partially altered cohenite crystals (highly reflective areas) in a matrix of nickeliferous goethite and maghemite (light grey regions)*
Top micrograph is at low magnification, scale bar = 1 mm
Bottom micrograph is at high magnification, scale bar = 500 µm.

Figure 5: *Sequence of reflected light micrographs of Mundrabilla from low to high magnification (a-c)*
Top micrograph is at low magnification, scale bar = 1 mm.

Middle micrograph is at medium magnification, scale bar = 500 µm

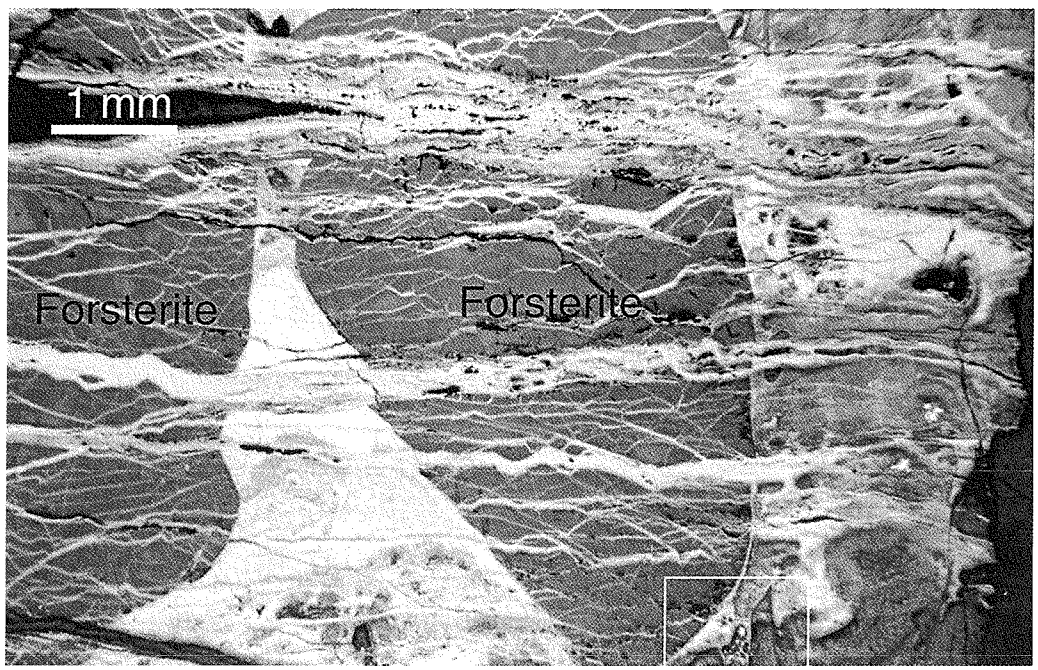

Bottom micrograph is at high magnification, scale bar = 100 μm. Highly reflective schreibersite fragments (white) are imbedded in a matrix of nickeliferous goethite (dark grey) and maghemite (light grey).

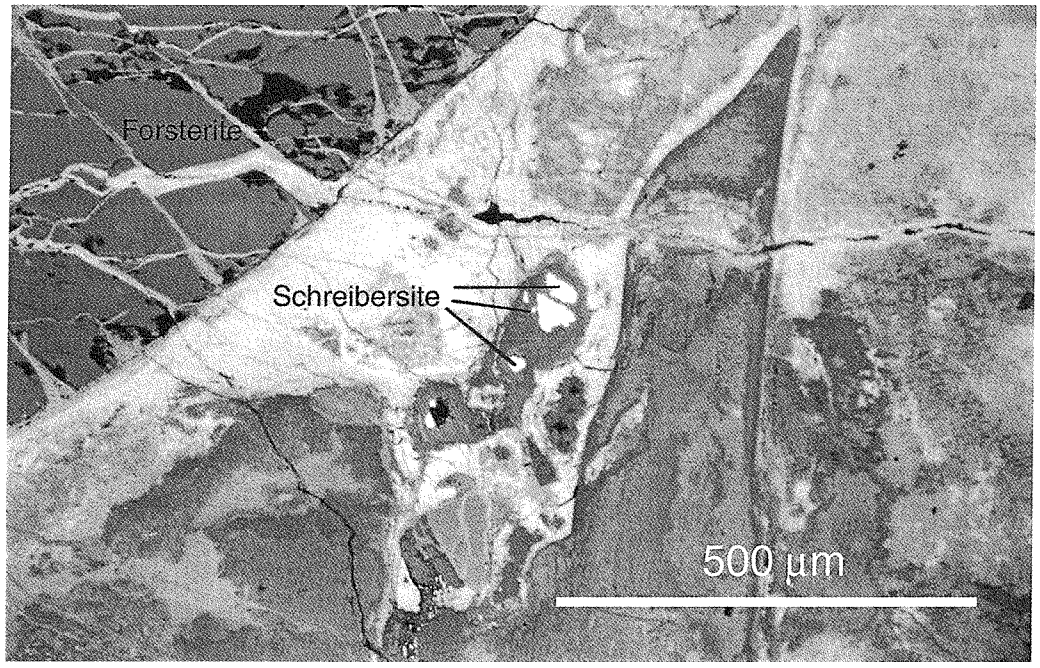

Figure 6: *Reflected light microscopy of Huckitta. Schreibersite and forsterite are indicated. Top micrograph is at low magnification, scale bar = 1 mm.*

Bottom micrograph is at high magnification, scale bar = 500 μm. Light grey patches are composed of nickeliferous goethite and maghemite.